COMPDYN 2013
4th ECCOMAS Thematic Conference on
Computational Methods in Structural Dynamics and Earthquake Engineering
M. Papadrakakis, V. Papadopoulos, V. Plevris (eds.)
Kos Island, Greece, 12–14 June 2013

NONSMOOTH ANALYSIS OF THE EARTHQUAKE-INDUCED POUNDING IN SKEW BRIDGES

Elias G. Dimitrakopoulos[1]

[1]Hong Kong University of Science and Technology
Department of Civil and Environmental Engineering, Kowloon, Clear Water Bay, Hong Kong
ilias@ust.hk

Keywords: skew bridges, oblique impact, unilateral contact, concrete bridges, linear complementarity problem, nonsmooth dynamics.

Abstract. *Skew bridges with separation/expansion joints are one of the most common types of existing bridges worldwide. Earthquake reconnaissance reports indicate that skew bridges often rotate in the horizontal plane, increasing the chances of unseating at their acute corners. This behaviour is triggered by the oblique, in-deck, contact which leads in coupling of the longitudinal and the transverse response, binding in one of the obtuse corners and subsequently rotation in the horizontal plane, in such a way that the skew angle increases. Despite the recorded evidence from previous earthquakes, and most empirical vulnerability methodologies, which acknowledge skew as a primary vulnerability factor of bridges, the relevant literature lacks a thorough theoretical study and is mostly confined to empirical descriptions of the phenomenon. This study examines both the case of deck-abutment impact, as well as, the impact between adjacent deck segments, of skew bridges. It shows that the coupling, and hence the unseating during an earthquake excitation, after deck-abutment collisions is not a factor of the skew angle alone, but rather of the total geometry in plan plus the contact parameters. Finally, it offers closed-form solutions for all physically feasible post-impact states observed in skew bridges.*

.

1 INTRODUCTION

The present paper examines the in-deck, as well as, the deck-abutment impact of skew bridges. On the same time, it belongs to a broader study [1]–[5] on the problem of the earthquake-induced pounding in (straight and skew) bridges. The aim of this research is to shed light on the impact-induced rotations in skew bridges deploying a nonsmooth dynamics methodology.

Skew bridges with expansion joints are one of the most common types of existing bridges worldwide. The recorded evidence from previous earthquakes [6] indicates that skew bridges often rotate (during earthquake excitation) in the horizontal plane, tending to drop off the supports at their acute corners [7] (Fig. 1). This behavior is triggered primarily by the oblique, impact at the expansion/separation joints and leads in coupling of longitudinal and transverse response, binding in one of the obtuse corners and subsequently rotation about that corner in such a way that the skew angle increases (Fig. 1).

The phenomenon of oblique multi-contact is the main gap in the existing knowledge regarding the seismic response of skew bridges. The recorded evidence from previous earthquakes and the empirical vulnerability methodologies that acknowledge skew as a primary vulnerability factor in bridges, create incentive to comprehend this mechanism. Impact in skew bridges has been primarily tackled with the contact element (or "compliance") approach [8], [9]. This study though, offers an in-depth analysis of the oblique and frictional impact of skew bridges within the context of nonsmooth dynamics. To this end, the study deploys a fully nonsmooth rigid body approach and uses set-valued force laws [10]. The proposed formulation captures all physically feasible impact states (such as multi-impact, multi-slip or stick) through a linear-complementarity problem.

The motivation for this research originates from (i) the need to elucidate the seismic response of skew bridges, (ii) the importance of this non-conventional behavior, manifested by empirical evidence, and (iii) the large number of existing bridges of this type worldwide.

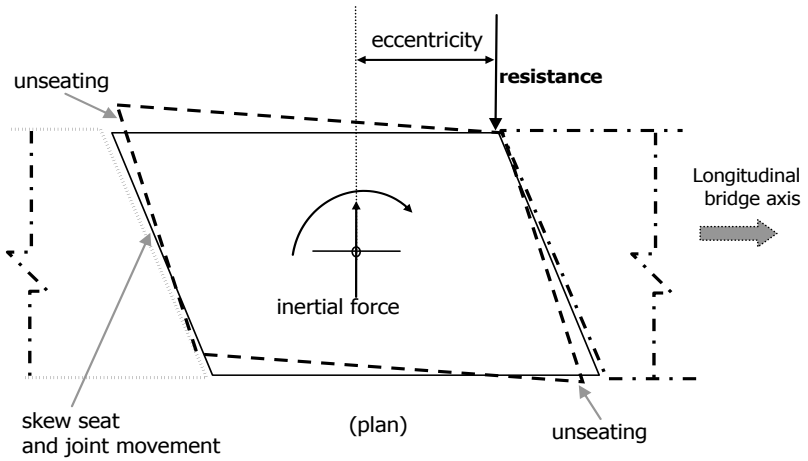

Figure 1: Rotation mechanism of skew bridges – potential unseating, adopted from [7].

2 PROPOSED NONSMOOTH DYNAMICS APPROACH

This study considers the individual bridge deck segments (in-between two successive separation/expansion joints) as rigid bodies moving on the horizontal plane and the abutments as inelastic half-spaces. The study further assumes that the interaction between adjacent segments, or between the deck and the abutment, is a unilateral contact and adopts the simplest impact laws, in a set-valued form [11], to describe this interaction.

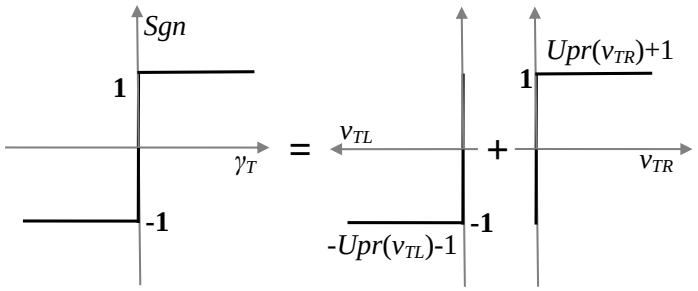

Figure 2: Set-valued friction force law.

In particular, the unilateral primitive *Upr* (e.g. Fig. 2, right) and Newton's coefficient of restitution $\varepsilon_N \in [0,1]$ describe the behavior in the normal direction of contact. A different set-valued map, the *Sgn*(x) function, enforces the Coulomb's friction law in the tangential direction of contact: $-\Lambda_{Ti} \in \mu_i \Lambda_{Ni}\,\mathrm{Sgn}\left(\gamma_{Ti}^{+}\right)$ where μ is the coefficient of friction and Λ_{Ti} the tangential impulse at contact *i*. The *Sgn*(x) function differs from the standard *sgn* function at the point x = 0, where the former yields a set of values: *Sgn*(*x* = 0) = [−1, 1], instead of a single value *sgn*(x = 0) = 0. Key role in this approach holds the decomposition of Fig. 2, which restores the complementarity conditions in the tangential direction of impact [4].

In integrated form the Newton – Euler equations are:

$$\mathbf{M}(\mathbf{u}^{+} - \mathbf{u}^{-}) = \mathbf{W}_{\mathrm{N}}\boldsymbol{\Lambda}_{\mathrm{N}} + \mathbf{W}_{T}\boldsymbol{\Lambda}_{T} \tag{1}$$

where $\mathbf{M}$ is the mass matrix and $\mathbf{W}$ are the direction matrices of the impulse vectors $\boldsymbol{\Lambda}$. Throughout this paper, superscript "+" refers to the post-impact state and super-script "–" to the pre-impact state, while sub-indexes *N, T* indicate the normal and the tangential direction of contact respectively. For the generalized velocities $\mathbf{u}$ and the generalized coordinates $\mathbf{q}$, $\dot{\mathbf{q}} = \mathbf{u}$ holds in an "*almost everywhere"* sense of functional analysis [11].

The relative (contact) velocities in the normal γ_N and the tangential γ_T direction are given by:

$$\begin{aligned} \boldsymbol{\gamma}_N^{+} - \boldsymbol{\gamma}_N^{-} &= \mathbf{G}_{NN}\boldsymbol{\Lambda}_{\mathrm{N}} + \mathbf{G}_{NT}\boldsymbol{\Lambda}_{T} \\ \boldsymbol{\gamma}_T^{+} - \boldsymbol{\gamma}_T^{-} &= \mathbf{G}_{TN}\boldsymbol{\Lambda}_{\mathrm{N}} + \mathbf{G}_{TT}\boldsymbol{\Lambda}_{T} \end{aligned} \tag{2}$$

where the "G" matrices are:

$$\begin{aligned} \mathbf{G}_{NN} &= \mathbf{W}_N^{T}\mathbf{M}^{-1}\mathbf{W}_{\mathrm{N}} \quad \mathbf{G}_{NT} = \mathbf{W}_N^{T}\mathbf{M}^{-1}\mathbf{W}_{T} \\ \mathbf{G}_{TN} &= \mathbf{W}_T^{T}\mathbf{M}^{-1}\mathbf{W}_{N} \quad G_{TT} = \mathbf{W}_T^{T}\mathbf{M}^{-1}\mathbf{W}_{T} \end{aligned} \tag{3}$$

Following the procedure outlined in [1], [4] the problem of the frictional multi-impact is formulated as a *linear complementarity problem* (LCP):

$$\begin{pmatrix} \mathbf{v}_N \\ v_{TR} \\ \Lambda_{TL} \end{pmatrix} = \begin{pmatrix} \mathbf{G}_{NN} - \mathbf{G}_{NT}\bar{\bar{\boldsymbol{\mu}}} & \mathbf{G}_{NT} & \mathbf{0} \\ \mathbf{G}_{TN} - G_{TT}\bar{\bar{\boldsymbol{\mu}}} & G_{TT} & 1 \\ 2\bar{\bar{\boldsymbol{\mu}}} & -1 & 0 \end{pmatrix} \begin{pmatrix} \boldsymbol{\Lambda}_N \\ \Lambda_{TR} \\ v_{TL} \end{pmatrix} + \begin{pmatrix} \left(\bar{\bar{\varepsilon}}_{\mathrm{N}} + \mathbf{E}\right)\boldsymbol{\gamma}_N^{-} \\ \gamma_T^{-} \\ 0 \end{pmatrix} \tag{4}$$

with the pertinent complementarity conditions being:

$$\begin{pmatrix} \mathbf{v}_N \\ v_{TR} \\ \Lambda_{TL} \end{pmatrix} \geq 0, \begin{pmatrix} \mathbf{\Lambda}_N \\ \Lambda_{TR} \\ v_{TL} \end{pmatrix} \geq 0, \quad \begin{pmatrix} \mathbf{v}_N \\ v_{TR} \\ \Lambda_{TL} \end{pmatrix}^T \begin{pmatrix} \mathbf{\Lambda}_N \\ \Lambda_{TR} \\ v_{TL} \end{pmatrix} = 0 \tag{5}$$

In which v_{TR} and v_{TL} are the right and left velocity-parts of the post-impact tangential velocity: $\gamma_{Ti}^{+} = v_{TRi} - v_{TLi}$, Λ_{TR} and Λ_{TL} are the corresponding impulses (Fig. 2) and $\mathbf{E}$ is the identity matrix. The proposed LCP (4), (5) encapsulates a great variety of impact states such as "slip", "stick", reversal of sign and nonimpulsive behaviour both for single-impact and multi (point)-impact (see section 4).

3 SKEW DECK-ABUTMENT IMPACT

The present section examines the different, deck-abutment, impact states that might occur within the deck of a skew bridge. The discussion starts from the (simpler) frictionless case, then focuses on double (point) frictional impact and finally summarizes single (point) impact as a special case of the pertinent double impact case. Section 4 presents, in a similar fashion, the in-deck impact of adjacent skew deck segments.

3.1 Double frictionless impact

When the pre-impact rotation is zero $\theta^{-}=0$ full-edge impact occurs between the deck (rigid body) and the abutment (inelastic half-space). Herein, full-edge impact (Fig. 3) is modeled (and referred to) as double impact due to the rigid body assumption.

In order to determine the unknown generalized velocities after impact, $\mathbf{u}^{+}$, one has to calculate first the corresponding impulses Λ_N. From Newton's impact law it follows that:

$$\mathbf{\Lambda}_N = -\mathbf{G}_{NN}^{-1}(\mathbf{E} + \bar{\bar{\boldsymbol{\varepsilon}}}_N)\boldsymbol{\gamma}_N^{-} \tag{6}$$

For the frictionless double impact of Fig. 3, Eqn (6) yields:

$$\begin{pmatrix} \dfrac{\Lambda_{N1}}{m\gamma_N^{-}} \\ \dfrac{\Lambda_{N2}}{m\gamma_N^{-}} \end{pmatrix} = -(1+\varepsilon_N) \begin{pmatrix} -\dfrac{r_2}{r_1 - r_2} \\ \dfrac{r_1}{r_1 - r_2} \end{pmatrix} = -\frac{(1+\varepsilon_N)}{2} \begin{pmatrix} 1-\eta_0 \\ 1+\eta_0 \end{pmatrix} \tag{7}$$

Equation (7) gives impulses Λ_{N1} and Λ_{N2} as a function of the geometry (α, L, W, *see* Fig. 3), the coefficient of restitution in the normal direction ε_N, and the translational mass m. However, Eqns.(7) are incomplete without the physical inequality constraint $\Lambda_N \geq 0$ which accounts for the unilateral nature of impact. Taking into account that by definition: $m(1+\varepsilon_N) > 0$, and that in order for contact to occur the relative velocity must be negative (which denotes an approach process), the sign of impulse depends solely on the dimensionless criterion, η_0, proposed in [1] which relates the ratio of the two sides in plan (L,W) with the skew angle, α, as follows:

$$\eta_0 = \frac{\sin 2\alpha}{2(W/L)} \tag{8}$$

For $\eta_0 > 1$, impulse at the acute corner is negative $\Lambda_{N1} < 0$ (Eqn.7), which violates the unilateral character of dry impact. The physical interpretation of a negative impulse, in this case, is that contact at that particular point is lost and hence the formulation of the impact problem

as double impact does not hold. Instead, when $\eta_0 > 1$, the impact problem should be treated as a single impact at the obtuse corner at which the impulse is always positive, $\Lambda_{N2} > 0$ (Eqn. 7). Hence, two distinct deck-abutment impact response patterns emerge: when $\eta_0 < 1$ (Fig. 3 top), the angular momentums of the two impulses Λ_{N1} and Λ_{N2} about the centre of mass (C.M.) are of a different sense and cancel out; as a consequence no (post-impact) angular velocity is developed [1]. On the contrary, when $\eta_0 > 1$ (Figure 6 bottom) impulse at the acute corner is lost, impact is effectively a single-impact, solely at the obtuse corner, and as a result angular velocity is developed due to impact. These observations unveil a complex, non-intuitive impact behavior that has not received the attention it deserves in relevant literature.

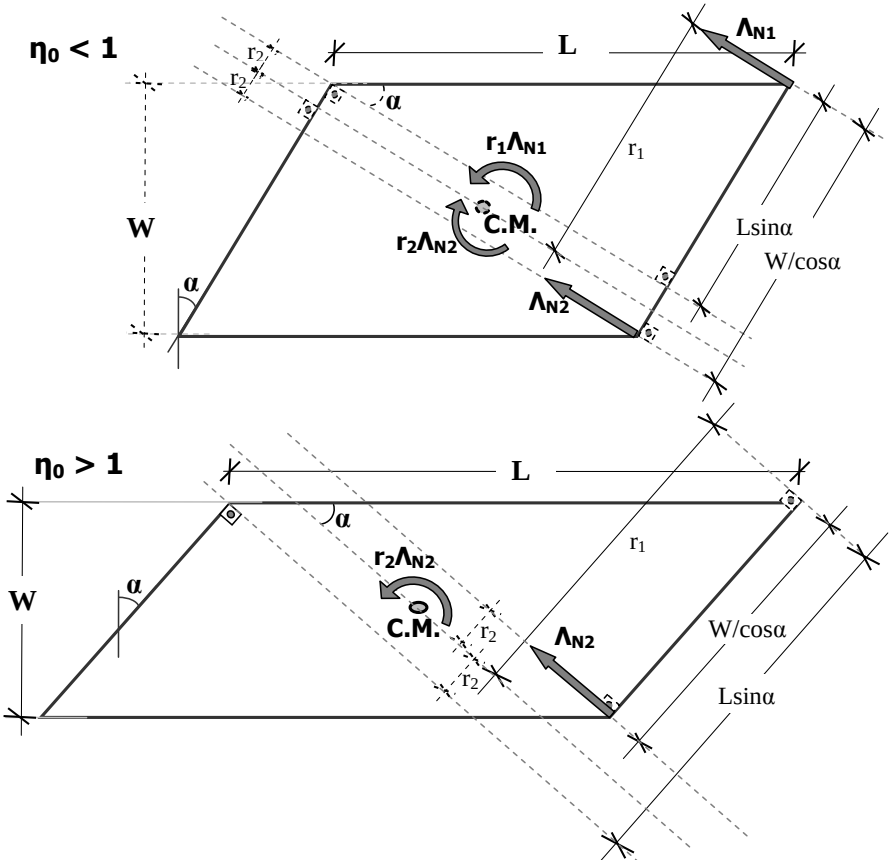

Figure 3: Geometry of the rocking masonry wall for (a) positive and (b) negative rotations.

3.2 Double frictional impact

In order to obtain a more realistic description of the deck-abutment impact of skew bridges, this section takes into account the presence of friction during impact. For the examined double frictional impact problem, the proposed LCP Eqns.(4 ,5) yields a great variety of potential solutions, in particular: three impact-states (backward slip, forward slip and stick) for each of the two contact points, when only one contact point is active (i.e. six single-impact states in total) and, in addition, three impact states when both contact points are active (double backward slip, double forward slip and double stick). Double impacts for which $\Lambda_N = 0$ holds at both impact points, lack physical interpretation and are not considered.

Friction perplexes the formulation of the double-impact problem of Fig. (3). The main difficulty lies in the linear dependency of the two impacts in the tangential direction, which

causes the appearance of singular matrices. The present study offers (in Section 4.2) a rational method to avoid the singularities arising from dependent constraints.

The response of the examined oblique frictional multi-impact configuration depends on (a) the geometry (in the form of the proposed dimensionless criterion η_0) and (b) on the kinematics (the tangential and the normal pre-impact velocity ratio) and the contact parameters (ε_N and μ). The former (a) determines if a contact point is active, while the latter (b) whether the double impact is forward/backward slip or stick.

The impulse and the tangential velocity for all physically feasible post-impact states can be summarized as follows:

Double slip: When double slip occurs $\Lambda_{N1} >0$, $\Lambda_{N2} >0$ and $\Lambda_T = \mp\mu\left(\Lambda_{N1}+\Lambda_{N2}\right)$, the impulses in the normal direction of the two (active) contact points are calculated from the LCP (Eqns. 4 and 5) as:

$$\begin{pmatrix} \dfrac{\Lambda_{N1}}{m\gamma_N^-} \\ \dfrac{\Lambda_{N2}}{m\gamma_N^-} \end{pmatrix} = \left(1+\varepsilon_{\mathrm{N}}\right) \begin{pmatrix} \dfrac{r_2 \pm \mu r_T}{r_1 - r_2} \\ \dfrac{r_1 \pm \mu r_T}{r_2 - r_1} \end{pmatrix} \tag{9}$$

The corresponding post-impact tangential velocity is (Eqns. 4 and 5):

$$\frac{\gamma_T^+}{\gamma_N^-} = \frac{1}{\varepsilon_N}\frac{\gamma_T^-}{\gamma_N^-} \pm \frac{-1-\varepsilon_N}{\varepsilon_N}\mu \tag{10}$$

In Eqns. (9) and (10) the positive sign (+) holds for backward slip and the negative sign (-) for forward slip.

Double stick: The impulses in the normal direction of the two (active) contact points ($\Lambda_{N1} >0$, $\Lambda_{N2} >0$) and the resultant impulse in the tangential direction $\left|\Lambda_T\right| < \mu\left(\Lambda_{N1}+\Lambda_{N2}\right)$ are given by Eqns. (20) (presented later in Section 4.2 and in [4]). The final expressions, which agree with the results of a different ad-hoc approach [1], are :

$$\begin{pmatrix} \dfrac{\Lambda_{N1}}{m\gamma_N^-} \\ \dfrac{\Lambda_{N2}}{m\gamma_N^-} \end{pmatrix} = \begin{pmatrix} \dfrac{r_T}{r_1 - r_2}\dfrac{\gamma_T^-}{\gamma_N^-} + \dfrac{r_2}{r_1 - r_2}\left(1+\varepsilon_N\right) \\ -\dfrac{r_T}{r_1 - r_2}\dfrac{\gamma_T^-}{\gamma_N^-} - \dfrac{r_1}{r_1 - r_2}\left(1+\varepsilon_N\right) \end{pmatrix} \text{ and } \frac{\Lambda_T}{m\gamma_N^-} = -\frac{\gamma_T^-}{\gamma_N^-} \tag{11}$$

Single slip: when impact takes place (solely) at the obtuse corner ($\Lambda_{N2} >0$, $\Lambda_{N1} =0$, and $\Lambda_T = \mp\mu\Lambda_{N2}$) the normal impulse is (Eqns. 4 and 5):

$$\frac{\Lambda_{N2}}{m\gamma_N^-} = -\frac{1+\varepsilon_N}{1+\dfrac{r_2^2 \pm \mu r_2 r_T}{I/m}} \tag{12}$$

Where I is the mass moment of inertia of the rigid body (deck-segment). Again in Eqns. (15) the positive sign (+) holds for backward slip and the negative sign (-) for forward slip. The corresponding post-impact tangential velocity is then:

$$\frac{\gamma_T^+}{\gamma_N^-} = \frac{\gamma_T^-}{\gamma_N^-} - \frac{r_2 r_T \pm \mu\left(I/m + r_T^2\right)}{I/m + r_2^2 \pm \mu r_2 r_T}\left(1+\varepsilon_N\right) \tag{13}$$

Note that backward slip at the acute corner ($\Lambda_{N1}>0$, $\Lambda_{N2}=0$, and $\Lambda_T = +\mu\Lambda_{N1}$) is not physically feasible [1].

Single Stick: When stick at the obtuse corner occurs ($\Lambda_{N2}>0$, $\Lambda_{N1}=0$, and $|\Lambda_T| < \mu\Lambda_{N2}$), the impulses in the normal and the tangential direction are (Eqns. 4 and 5):

$$\frac{\Lambda_{N2}}{m\gamma_N^-} = \frac{-\left(I/m + r_T^2\right)\left(1+\varepsilon_N\right) + r_2 r_T \dfrac{\gamma_T^-}{\gamma_N^-}}{I/m + r_2^2 + r_T^2} \qquad \frac{\Lambda_T}{m\gamma_N^-} = \frac{r_2 r_T\left(1+\varepsilon_N\right) - \left(I/m + r_2^2\right)\dfrac{\gamma_T^-}{\gamma_N^-}}{I/m + r_2^2 + r_T^2} \tag{14}$$

Slip/stick at the acute corner is described also by Eqns. (12 and 13)/(14 and 15) substituting lever r_2 with lever r_1.

3.3 Single frictional impact

When the pre-impact rotation of the rigid body (deck-segment) is non-zero, single point impact takes place. The proposed LCP (Eqns. 4, 5) describes also single frictional impacts, as a special case when only one impact point is active (i.e. $\Lambda_N > 0$ holds at that point). In particular, the closed-form solutions of Section 3.2 for single-impacts hold provided the appropriate levers r_1, r_2 and r_T are used. Figure 4 presents sample results of the existential conditions of the three distinct (single) impact states (forward slip, backward slip and stick).

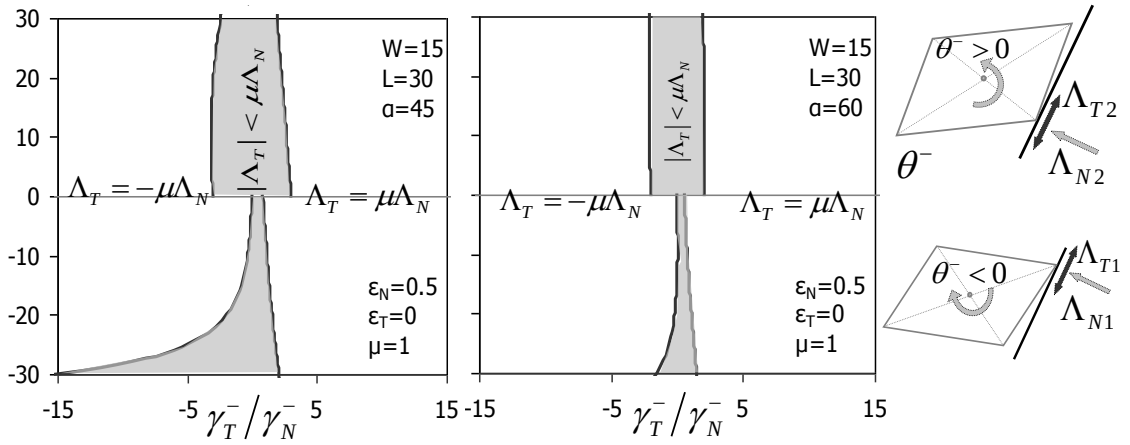

Figure 4: The three distinct single frictional impact states in the $\gamma_T^-/\gamma_N^-, \theta^-$ plane for coefficient of restitution $\varepsilon_N = 0.5$, skew angle $\alpha = 45^o$ (left), 60^o (right), coefficient of friction $\mu = 1$.

4 IN-DECK SKEW BRIDGE IMPACT

This section describes the impact between two adjacent skew bridge-segments (Fig. 5). A detailed discussion of the kinematics of a pair of skew rigid bodies (adjacent deck segments) is offered in [4]. The present study though focuses on the description of the physically feasible post-impact conditions for the configuration of Fig. 5.

4.1 Double frictionless impact

Again, utilizing the rigid body assumption, full-edge impact is modeled as a double-point impact and the discussion starts with the frictionless case. With reference to Fig. 5, full-edge contact occurs when the two bodies come to contact while their pre-impact rotations are the same $\theta_1^- = \theta_2^-$. In the following, without loss of generality it is as assumed that: $\theta_1^- = \theta_2^- = 0$.

Inequalities (16) give the conditions under which the sign of the two point impulses is positive, or in other words, the corresponding contact point is active.

$$\begin{aligned} \Lambda_{N1} > 0 &\Rightarrow \frac{I_1}{I_2} > \frac{\eta_1 - 1}{\eta_2 + 1} \\ \Lambda_{N2} > 0 &\Rightarrow \frac{I_2}{I_1} > \frac{\eta_2 - 1}{\eta_1 + 1} \end{aligned}, \quad \eta_j = \frac{\sin 2\alpha}{2\left(W/L_j\right)}, \quad j = 1,2 \tag{15}$$

Compared with the case of (skew) deck- abutment impact (Fig. 3), the impact mechanism of in-deck impact (Fig. 5) is considerably more complicated. In particular, the signs of the impulses depend not only on the geometry (the proposed dimensionless criteria η_1, η_2), but also on the ratio of the mass moments of inertial of the two bodies I_1/I_2. A simple parametric analysis shows that in most cases of practical interest both contact points are active. The solution of the Newton-Euler equations (1) shows that, unlike the deck-abutment case, in-deck double impact causes both rigid bodies (deck-segments) to rotate in the direction of increasing the skew angle, but with equal post-impact angular velocities. However, when impact is effectively single-point impact the two bodies develop different post-impact angular velocities and hence different rotations.

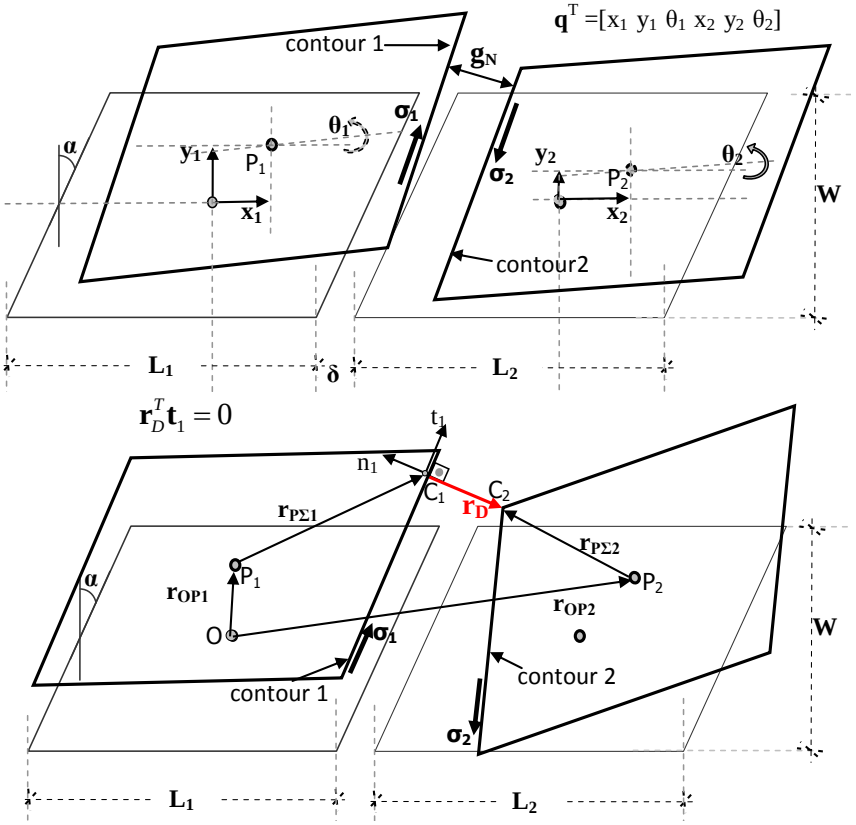

Figure 5: Geometry of two planar rigid bodies – simulating adjacent skew bridge segments.

4.2 Double frictional impact

Consider the frictional full-edge impact of two adjacent skew deck segments (Fig. 6). The "conventional" simulation approach is to consider the normal and the tangential impulses of each contact point explicitly: $\mathbf{\Lambda}_T = \left(\Lambda_{T1} \quad \Lambda_{T2}\right)^T$. This formulation of the double impact problem, neglects that the two (point) impacts are linearly dependent in the tangential direction and, as a consequence $\mathbf{G}_{NT}$, $\mathbf{G}_{TN}$ and $\mathbf{G}_{TT}$ (3) are all singular matrices (of size 2x2). This is a typical case of overconstrainted impacts which arise often in multibody dynamics with multi-contacts. The present study proposes an alternative description of the double impact, which does not over-constrain the problem and, on the same time, allows for a closed-form solution avoiding all singularities during solution of the LCP. Instead of examining the tangential impulse in each point explicitly, the proposed simulation considers solely the resultant (scalar) tangential impulse Λ_T (Fig. 6) resulting in $\mathbf{G}_{NT} = \mathbf{G}_{TN}^T$, $\mathbf{G}_{NT} \in \mathbb{R}^{2\times 1}$, $\mathbf{G}_{TN} = \mathbf{G}_{NN}^T \in \mathbb{R}^{1\times 2}$ and $G_{TT} \in \mathbb{R}^{1\times 1}$.

Again, two conditions govern the post-impact state of the frictional multi-impact problem of Fig. 6: (i) the geometrical and inertial properties determine which contact points are active (the pertinent normal impulse is positive $\Lambda_N > 0$) and (ii) the kinematical conditions together with the contact parameters (ε_N and μ) determine whether the impact results in (forward/backward) slip or stick.

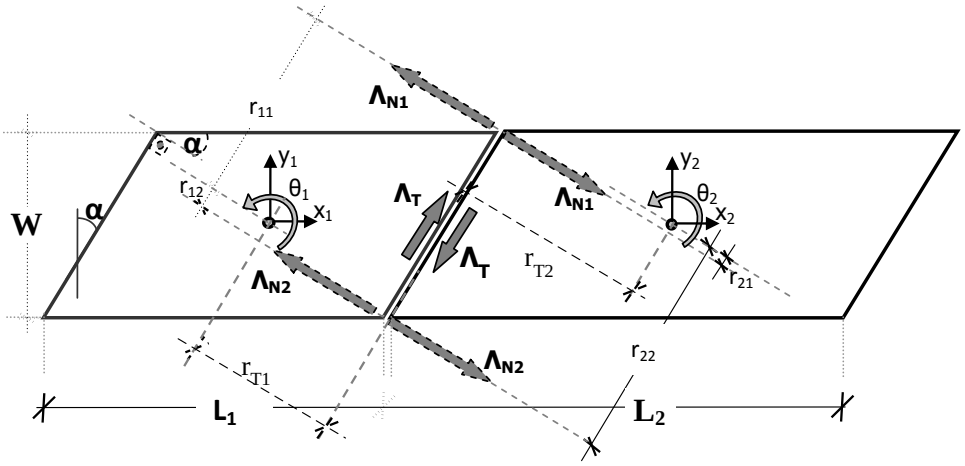

Figure 6: Full-edge frictional impact between two skew deck segments (considered as rigid bodies).

Double slip: with reference to Fig.6 (which shows levers r_{11}, r_{12}, r_{21}, r_{22}, r_{T1} and r_{T2}) the impulses in the normal direction of the two (active) contact points are (Eqns. 4 and 5):

$$\begin{pmatrix} \dfrac{\Lambda_{N1}}{\gamma_N^- M} \\ \dfrac{\Lambda_{N2}}{\gamma_N^- M} \end{pmatrix} = -\left(1+\varepsilon_N\right) \begin{pmatrix} \dfrac{\left(r_{12}-r_{11}\right)\left(r_{12} \pm \mu r_{T1}\right)}{I_1} + \dfrac{\left(r_{22}-r_{21}\right)\left(r_{22} \pm \mu r_{T2}\right)}{I_2} \\ \dfrac{\left(r_{11}-r_{12}\right)\left(r_{11} \pm \mu r_{T1}\right)}{I_1} + \dfrac{\left(r_{21}-r_{22}\right)\left(r_{21} \pm \mu r_{T2}\right)}{I_2} \end{pmatrix} \tag{16}$$

Where I_1, I_2 are the mass moment of inertias of the two bodies (deck-segments). The corresponding post-impact tangential velocity is:

$$\frac{\gamma_T^+}{\gamma_N^-}=\frac{\gamma_T^-}{\gamma_N^-}-(1+\varepsilon_N)M\left\{\begin{array}{l}\dfrac{\mu}{\bar{m}}\left[\dfrac{(r_{11}-r_{12})^2}{I_1}+\dfrac{(r_{21}-r_{22})^2}{I_2}\right]+\\ \dfrac{1}{I_1I_2}\left[(r_{21}-r_{22})r_{T1}+\right]\left[\begin{array}{l}(r_{21}-r_{22})\mu r_{T1}+\\ (r_{12}-r_{11})\mu r_{T2}\pm(r_{12}r_{21}-r_{11}r_{22})\end{array}\right]\end{array}\right\} \tag{17}$$

Where $\bar{m}=\dfrac{m_1m_2}{m_1+m_2}$ and:

$$\frac{1}{M}=\frac{1}{\bar{m}}\left[\frac{(r_{11}-r_{12})^2}{I_1}+\frac{(r_{21}-r_{22})^2}{I_2}\right]+\frac{r_{12}r_{21}-r_{11}r_{22}}{I_1I_2}\left[\begin{array}{l}\pm(r_{21}-r_{22})\mu r_{T1}\pm(r_{12}-r_{11})\mu r_{T2}\\ +r_{12}r_{21}-r_{11}r_{22}\end{array}\right] \tag{18}$$

In Eqns. (17) to (19) the positive sign (+) holds for backward slip and the negative sign (-) for forward slip respectively.

Double stick: When $\Lambda_{N1}>0$, $\Lambda_{N2}>0$ and $|\Lambda_T|<\mu(\Lambda_{N1}+\Lambda_{N2})=\bar{\bar{\boldsymbol{\mu}}}\boldsymbol{\Lambda}_N$, double stick takes place and the corresponding post-impact velocities are zero. The impulses in the normal direction of the two (active) contact points and the resultant impulse in the tangential direction are (Eqns. 4 and 5):

$$\begin{aligned}\boldsymbol{\Lambda}_N&=\frac{1}{G_{TT}-\mathbf{G}_{TN}\mathbf{G}_{NN}^{-1}\mathbf{G}_{NT}}\left[\mathbf{G}_{NN}^{-1}\mathbf{G}_{NT}\gamma_T^--\left[\begin{array}{l}\mathbf{G}_{NN}^{-1}\mathbf{G}_{NT}\mathbf{G}_{TN}+\\ \left(G_{TT}-\mathbf{G}_{TN}\mathbf{G}_{NN}^{-1}\mathbf{G}_{NT}\right)\mathbf{E}\end{array}\right]\mathbf{G}_{NN}^{-1}\left(\bar{\bar{\varepsilon}}_N+\mathbf{E}\right)\boldsymbol{\gamma}_N^-\right]\\ \Lambda_T&=\frac{\mathbf{G}_{TN}\mathbf{G}_{NN}^{-1}\left(\bar{\bar{\varepsilon}}_N+\mathbf{E}\right)\boldsymbol{\gamma}_N^--\gamma_T^-}{G_{TT}-\mathbf{G}_{TN}\mathbf{G}_{NN}^{-1}\mathbf{G}_{NT}}\end{aligned} \tag{19}$$

Single slip: When slip takes place at point 1 (solely) the normal impulse is (Eqns. 4 and 5):

$$\frac{\Lambda_{N1}}{\bar{m}\gamma_N^-}=-\frac{1+\varepsilon_N}{1+\dfrac{r_{11}^2\pm\mu r_{11}r_{T1}}{I_1/\bar{m}}+\dfrac{r_{21}^2\pm\mu r_{21}r_{T2}}{I_2/\bar{m}}} \tag{20}$$

Whereas the tangential post-impact velocity is given by (Eqns. 4 and 5):

$$\frac{\gamma_T^+}{\gamma_N^-}=\frac{\gamma_T^-}{\gamma_N^-}-\frac{\pm\dfrac{\mu}{\bar{m}}+\dfrac{r_{11}r_{T1}\pm\mu r_{T1}^{\ 2}}{I_1}+\dfrac{r_{21}r_{T2}\pm\mu r_{T2}^{\ 2}}{I_2}}{\dfrac{1}{\bar{m}}+\dfrac{r_{11}^2-\mu r_{11}r_{T1}}{I_1}+\dfrac{r_{21}^2-\mu r_{21}r_{T2}}{I_2}}(1+\varepsilon_N) \tag{21}$$

Again, sign (+) holds for backward slip and sign (-) corresponds to forward slip. For impact at point 2 one has to replace levers r_{12} and r_{22} with r_{11} and r_{21} respectively.

Single stick: When stick occurs at point 1 (Fig.6) the normal and tangential impulses are:

$$\frac{\Lambda_{N1}}{\bar{m}\gamma_N^-}=\frac{1}{\bar{m}}\frac{\left(\frac{r_{11}r_{T1}}{I_1}+\frac{r_{21}r_{T2}}{I_2}\right)\frac{\gamma_T^-}{\gamma_N^-}-\left(\frac{1}{\bar{m}}+\frac{r_{T1}{}^2}{I_1}+\frac{r_{T2}{}^2}{I_2}\right)\left(1+\varepsilon_N\right)}{\left(\frac{1}{\bar{m}}+\frac{r_{11}^2}{I_1}+\frac{r_{21}^2}{I_2}\right)\left(\frac{1}{\bar{m}}+\frac{r_{T1}{}^2}{I_1}+\frac{r_{T2}{}^2}{I_2}\right)-\left(\frac{r_{11}r_{T1}}{I_1}+\frac{r_{21}r_{T2}}{I_2}\right)^2}$$

$$\frac{\Lambda_{T}}{\bar{m}\gamma_N^-}=\frac{1}{\bar{m}}\frac{\left(\frac{r_{11}r_{T1}}{I_1}+\frac{r_{21}r_{T2}}{I_2}\right)\left(1+\varepsilon_N\right)-\left(\frac{1}{\bar{m}}+\frac{r_{T1}{}^2}{I_1}+\frac{r_{T2}{}^2}{I_2}\right)\frac{\gamma_T^-}{\gamma_N^-}}{\left(\frac{1}{\bar{m}}+\frac{r_{11}^2}{I_1}+\frac{r_{21}^2}{I_2}\right)\left(\frac{1}{\bar{m}}+\frac{r_{T1}{}^2}{I_1}+\frac{r_{T2}{}^2}{I_2}\right)-\left(\frac{r_{11}r_{T1}}{I_1}+\frac{r_{21}r_{T2}}{I_2}\right)^2} \tag{22}$$

Where $\bar{m}=m_1m_2/\left(m_1+m_2\right)$. For impact at point 2 (Fig.6) one has to replace levers r_{12} and r_{22} with r_{11} and r_{21} respectively.

4.3 Single frictional impact

When the pre-impact rotations of the two rigid bodies (deck-segments) are different, single point impact takes place. Again, the proposed LCP (Eqns. 4, 5) describes also single frictional impacts, as a special case when only one impact point is active (i.e. $\Lambda_N > 0$ holds at that point). In particular, the closed-form solutions of Section 4.2 for single-impacts hold provided the appropriate levers r_{11}, r_{21}, r_{21}, r_{22}, r_{T1} and r_{T2} are used [4].

5 CONCLUSIONS

The aim of the present paper is to bring forward the impact mechanism during in-deck collisions in skew bridges. To this end, the study adopts a fully nonsmooth rigid body approach and examines in depth the impact response of a planar skew (rigid) body against an inelastic half-space, as well as, the impact of a pair of planar rigid bodies. Key features of the present approach are the proposed linear complementarity problem, which encapsulates all physically feasible impact states, and the use of set-valued force laws.

The analysis of the rotation mechanism associated with oblique impact shows that the tendency of skew bridges to rotate depends on the total geometry of the body in plan, and not on the skew angle alone, as it is commonly considered. In addition, the post-impact state depends on the contact parameters, the inertial properties of the two segments (for impact between adjacent deck segments) and on the pre-impact kinematics. Further, the study elaborates on the conditions under which oblique (frictionless or frictional) impact triggers deck rotation in skew bridges. It shows that post-impact rotation is more common for impact between adjacent deck-segments than deck-abutment impact. It also verifies that in most cases, post-impact rotation is in the direction of increasing the skew angle. For each physically feasible impact state (single slip/stick at either corner of a skew deck segment, or double slip/stick along the whole edge of a segment), it offers pertinent closed-form solutions which yield the unknown impulses in the normal and the tangential direction of contact and the post-impact velocities when the latter are unknown (slip post-impact states).

ACKNOWLEDGEMENTS

The author gratefully acknowledges the financial support for this research provided by the Research Grants Council of Hong Kong, under grant reference number DAG12EG03.

REFERENCES

[1] E. G. Dimitrakopoulos, Analysis of a Frictional Oblique Impact Observed in Skew Bridges, *Nonlinear Dynamics*, **60**, 575–595, 2010.

[2] E. G. Dimitrakopoulos, N. Makris, and A. J. Kappos, Dimensional analysis of the earthquake-induced pounding between inelastic structures, *Bulletin of Earthquake Engineering*, **9**(2), 561–579, 2011.

[3] E. G. Dimitrakopoulos, Seismic response analysis of skew bridges with pounding deck–abutment joints, *Engineering Structures*, **33**(3), 813–826, 2011.

[4] E. G. Dimitrakopoulos, Nonsmooth Analysis of the Impact Between Successive Skew Bridge-segments, *Nonlinear Dynamics*, **under review 2013**.

[5] E. G. Dimitrakopoulos, N. Makris, and A. J. Kappos, Dimensional analysis of the earthquake-induced pounding between adjacent structures, *Earthquake Engineering Structural Dynamics*, **38**(7), 867–886, 2009.

[6] A. S. Elnashai, B. Gencturk, O.-S. Kwon, Y. M. A. Hashash, S. J. Kim, S.-H. Jeong, and J. Dukes, The Maule (Chile) earthquake of February 27, 2010: Development of hazard, site specific ground motions and back-analysis of structures, *Soil Dynamics and Earthquake Engineering*, **42**, 229–245, 2012.

[7] M. J. N. Priestley, G. M. Calvi, and F. Seible, *Seismic design and retrofit of bridges*. Wiley, 1996.

[8] Y. Huo and J. Zhang, Effects of Pounding and Skewness on Seismic Responses of Typical Multi-Span Highway Bridges Using Fragility Function Method, *Journal of Bridge Engineering*, doi:10.1061/(ASCE)BE.1943-5592.0000414.

[9] P. Kaviani, F. Zareian, and E. Taciroglu, Seismic behavior of reinforced concrete bridges with skew-angled seat-type abutments, *Engineering Structures*, **45**, 137–150, 2012.

[10] C. Glocker, *Set-valued force laws : dynamics of non-smooth systems*. Springer, 2001.

[11] M. Payr and C. Glocker, Oblique Frictional Impact of a Bar: Analysis and Comparison of Different Impact Laws, *Nonlinear Dynamics*, **41**(4), 361–383, 2005.